

Document downloaded from:

<http://hdl.handle.net/10251/60369>

This paper must be cited as:

Carpio, P.; Blochet, Q.; Pateyron, B.; Pawlowski, L.; Salvador Moya, MD.; Borrell Tomás, MA.; Sanchez, E. (2013). Correlation of thermal conductivity of suspension plasma sprayed yttria stabilized zirconia coatings with some microstructural effects. *Materials Letters*. 107:370-373. doi:10.1016/j.matlet.2013.06.051.



The final publication is available at

<http://dx.doi.org/10.1016/j.matlet.2013.06.051>

Copyright Elsevier

Additional Information

Manuscript Number:

Title: Correlation of thermal conductivity of suspension plasma sprayed yttria stabilized zirconia coatings with some microstructural effects

Article Type: Letter

Keywords: Thermal barrier coatings; Suspension plasma spraying; Thermal conductivity; Coating microstructure

Corresponding Author: Mr. Pablo Carpio,

Corresponding Author's Institution: Instituto de Tecnología Cerámica.
Universitat Jaume I

First Author: Pablo Carpio

Order of Authors: Pablo Carpio; Quentin Blochet; Bernard Pateyron; Lech Pawłowski; Maria Dolores Salvador; Amparo Borrell; Enrique Sanchez, Ph.D.

Abstract: Yttria-stabilized zirconia (3YSZ) coatings were successfully obtained by suspension plasma spraying. The coatings present generally two-zones-microstructure comprising nanostructured zones contributed by unmolten, partially sintered nanoparticles sintered surrounded by lamellar splats formed from molten and agglomerated in-flight fine solids. In addition, different types of cracks inside the coating microstructure were classified and quantified by image analysis such as e.g. inner microcracks and segmentation cracks associated with quenching process as well as horizontal interlamellar cracks. Thermophysical properties of sprayed coatings were tested with a thermal diffusivity set up basing onto light flash principle. Subsequently, the thermal conductivity was determined with the use of literature data of density and specific heat. The calculations showed very low thermal conductivities values. The values did not correlate with coatings porosity data. Consequently, the analysis of variance (ANOVA) test allowed evaluating the possible impact of the various types of cracks on thermal conductivity. By this analysis, a good correlation between vertical cracks, which include microcracks and segmentation cracks, and thermal conductivity was found. The findings also confirmed the increase of thermal conductivity associated with this type of cracks.

Suggested Reviewers: Irene G Cano PhD
Project Manager, Centre de Proyecció Térmica (CPT), Universidad de Barcelona
igcano@cptub.eu

She is a researcher with a long trajectory about thermal spray

Luca Lusvargui PhD

University Researcher, Dipartimento di Ingegneria dei Materiali e
dell'Ambiente, Università degli Studi di Modena e Reggio Emilia
luca.lusvargui@unimore.it
He is a researcher with a long trajectory about APS and HVOF coatings.

Geoffrey Darut PhD
Researcher, LERMPS, Université de Technologie de Belfort-Montbéliard
geoffrey.darut@utbm.fr
He is a researcher with a trajectory about SPS coatings.

Highlights:

1. YSZ coatings were deposited by SPS from commercial nanosuspension.
2. Different kind of cracks was identified.
3. Thermal diffusivity was measured by lamp flash method.
4. Coatings with very low thermal conductivity were obtained.
5. A good correlation between vertical cracks and thermal conductivity was found.

1. Introduction

1 Thermal barrier coatings (TBCs) are employed to protect the metallic components against corrosion and
2 oxidation at high temperature. Atmospheric plasma spraying (APS) is one of the most popular technologies
3 to obtain TBCs because of its flexibility and low cost [1]. The material of TBCs is currently yttria-stabilized
4 zirconia (YSZ) due to its low thermal conductivity, relatively low coefficient of thermal expansion, phase
5 stability and high corrosion resistance [2]. The increase in the operational temperature of gas turbines
6 resulted in the demand to find coatings enabling better thermal isolation [3]. Consequently, an intense
7 research activity has started to reduce the thermal conductivity of TBCs [4,5,6]. In general, high porosity
8 associated with cracks in the coating results in low thermal conductivity, but the shape of pores and cracks
9 and their size distribution may also influence considerably this parameter.

10 More recent research has focused on the use of nanostructured feedstocks [7] and they have demonstrated that
11 the nanostructured coatings have lower thermal conductivity than that of their conventional counterparts,
12 basically due to the presence of unmolten and porous nano-zones.

13 One way of obtaining nanostructured coatings consists of using a carrier liquid to inject a suspension of
14 nanoparticles inside the plasma instead of dry powder. This process, known as suspension plasma spraying
15 (SPS), has undergone extensive development in the last years due to the fact that the feedstock preparation
16 process is much easier than that of agglomeration of nanostructured solids by spray-drying. SPS coatings
17 with improved properties, in comparison with those of coatings obtained from conventional (microstructured)
18 APS feedstocks, have been reported [8]. The previous research has also shown that TBCs obtained by SPS
19 exhibit very low thermal conductivity and higher thermal shock resistance without substantially varying the
20 hardness or elastic modulus [9]. However there are only very few studies which investigate qualitatively the
21 relationship between microstructure and thermal conductivity [10].

22 From the above it can be deduced that nanostructured YSZ coatings obtained with the use of SPS process
23 have the potential to become part of the next generation of TBCs. Nevertheless, there is a need to
24 quantitatively assess the relationship between microstructure and thermal conductivity by modeling
25 important microstructural features. Thus the present research addresses a first attempt to present a simple,
26 quantified correlation between the cracks present in YSZ SPS coatings and thermal conductivity. The
27 coatings described in this work were obtained and characterized in our previous study [11].

2. Experimental

2.1. Materials and coating deposition

A commercial aqueous suspension of 3 mol% yttria-stabilized zirconia (YSZ) nanoparticles (MELox Nanosize 3Y, Mel Chemicals, United Kingdom) was deposited on AISI 304 stainless steel specimens by suspension plasma spraying (SPS). The coatings were obtained in a set of experiments following a factorial model which aimed to addressing the effect of the operational spray parameters on microstructure and mechanical properties of the sprayed coatings. The studied parameters are displayed in Table 1 and procedure details can be viewed at [11].

2.2. Coating characterization

The coating's cross-sections were characterized by field emission scanning electron microscopy (FEG-SEM, S-4800, Hitachi, SCSIE of the University of Valencia). In addition, the different types of cracks present in the coatings were identified and quantified by image analyzer (Visilog 5.3, Noesis S.A.). In order to obtain a representative, complete scan of the entire cross-sectional area, 10 FEG-SEM backscattered electron micrographs were analyzed (x1000 magnification) for each sample. Phase identification by X-ray diffraction as well as mechanical properties (hardness and elastic modulus) by nanoindentation are described elsewhere [11].

Thermal conductivity was calculated from the following equation:

$$\lambda(T) = \alpha(T) \cdot c_p(T) \cdot \rho \quad (1)$$

in which λ is thermal conductivity in W/(m·K), α is thermal diffusivity in m²/s, c_p is specific heat in J/(kg·K) and ρ is apparent density of the coating at room temperature in kg/m³. The specific heat was calculated by differential calorimetric technique following the equation:

$$c_p(T) = \frac{1}{m_g} \cdot \frac{\Delta H}{\Delta T} \quad (2)$$

in which ΔH is the enthalpy in J, ΔT is the temperature variation in K and m_g is the amount of free-standing coating in kg.

The coating porosity, which was also determined from the image analysis procedure set out above, was taken into account in order to determine the coating density. The coating density was calculated from the following expression:

$$\rho = \rho_0 \cdot (1 - P) \quad (3)$$

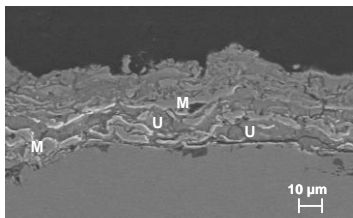
1
2 in which ρ_0 is the non-porous material density of YSZ which was estimated on 5890 kg/m^3 [12] and P is the
3 porosity.

4 The thermal diffusivity measurements were performed by lamp flash method using LFA 447 NanoFlash[®]
5 Flash Lamp System (Netzsch, Germany). The setup enables measurements in the temperature range from
6 room temperature to 573 K in air.
7

8
9 The possible impact of the various types of cracks on thermal conductivity was studied. The correlations
10 were ratified by analysis of variance (ANOVA) method. Test F was performed in which critical F value
11 means the probability to exist a significant influence between the thermal conductivity and the considered
12 parameters. When critical F value is lower than 0.05 the correlation is valid. In contrast, when critical F
13 exceeds 0.05, the correlation is not valid and the number of parameters must be changed in order to reduce
14 critical F.
15
16
17
18
19
20
21

22 3. Results and Discussion

23
24 Cross-sectional FEG-SEM images of one of the as-sprayed coatings is shown in Fig. 1. The figure reveals the
25 two-zone microstructure which consists of nanostructured zones formed by unmolten nanoparticles (marked
26 U in Fig.1) surrounded by lamellar (splats), molten powder matrix (marked M in this figure). Similar
27 microstructures were observed in the rest of the coatings which correspond to those reported in the literature
28 for SPS-YSZ coatings [7].
29
30
31
32
33



34
35
36
37
38
39
40
41 **Figure 1.**

42
43 The arrows in Fig. 2 show that different types of cracks can be distinguished in the coatings as reported
44 elsewhere [4,13]. On the one hand, several microcracks are produced in the direction normal to the substrate.
45 These intra-splats cracks appearing through coating's thickness could have been generated during splat
46 quenching (*inner cracks*). Some of them grow from the bond coat-top coat interface to surface top coat
47 (*segmentation cracks*) and may affect the mechanical and thermal properties [14]. On the other hand, the
48 third type of cracks evolves parallel to the substrate at the molten grains boundaries (*inter-splats*) indicating
49 somehow poor lamellae cohesion (*horizontal cracks*). This crack morphology is depicted in Figure 2 together
50 with the original micrograph where the actual cracks come from. The percentage of each type of crack
51 assessed by image analysis is shown in Table 1.
52
53
54
55
56
57
58
59
60
61
62
63
64
65

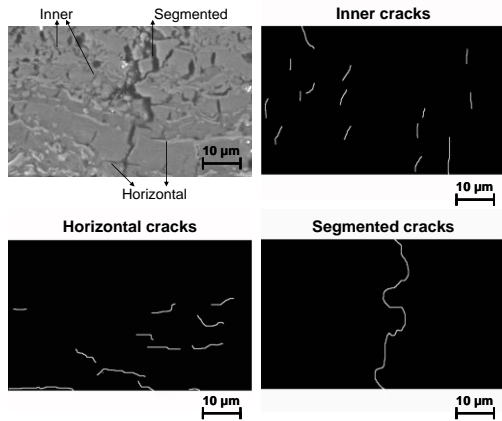


Figure 2.

Thermal diffusivity at different temperatures as well as specific heat and porosity were measured in order to calculate the thermal conductivity, which is also showed in Table 1.

As previously mentioned, the TBCs coatings obtained by SPS process exhibit very low thermal conductivities (typically 0.6-0.8 W/m·K) being lower than those of the coatings obtained by conventional atmospheric plasma spray (APS) process (usually between 0.8-1.2 W/m·K). According to Table 1, the samples 2, 3 and 4 had the smallest thermal conductivity. The sample 3 displayed an extremely low thermal conductivity of $\lambda=0.43$ W/m·K at 573 K. The explication of such low thermal conductivity in YSZ SPS coatings can be the peculiar pore network architecture mainly made up of nanometric-sized pores [15]. In addition, this pores network is difficult to quantify using conventional techniques due to their low resolution. In the present research porosity values (determined from FEG-SEM images) ranged from 6 % \pm 1 to 8 % \pm 1 which correspond to typical SPS coatings. Despite the difficulty in quantifying this porosity, the significant differences in thermal conductivity among the coatings confirm the strong dependence of this characteristic with the coatings microstructural features.

Different correlations, according to the types of cracks set out in Fig. 2 were attempted. Correlation coefficient (R^2) and critical F of these correlations are detailed in Table 2.

First, in case 1, each type of crack (*inner*, *segmentation* and *horizontal*) was analyzed separately. Although correlation coefficient is higher than 0.9, critical F value exceeds 0.05 in all the cases therefore the correlation is invalid. This is because only one degree of freedom is taken into account. For this reason, the number of parameters was reduced in order to increase the degrees of freedom.

For this purpose, in case 2, *inner* and *segmentation* cracks were linked in the same type of crack now called *vertical* cracks. In fact as reported elsewhere *segmentation* cracks develop from inner cracks when a low energy release rate is promoted during splat quenching [16]. Thus SPS coatings form easily segmentation cracks due to the low energy release rate associated with their thinner splats [14]. Critical F was still higher

1
2
3
4
5
6
7
8
9
10
11
12
13
14
15
16
17
18
19
20
21
22
23
24
25
26
27
28
29
30
31
32
33
34
35
36
37
38
39
40
41
42
43
44
45
46
47
48
49
50
51
52
53
54
55
56
57
58
59
60
61
62
63
64
65

than 0.05 but lower than that of the first case. Moreover, relative error as worked out from correlation coefficients was very high, in particular the contribution to this error by *horizontal* cracks. Again the correlation was weak.

Finally, in case 3, only *vertical* cracks (sum of inner and *segmentation* cracks) were considered. Critical F value was lower than 0.05 with an acceptable error what indicates that a correlation between *vertical* cracks and thermal conductivity does exist. A positive correlation number means that a higher *vertical* cracks density gives rise to an increase of thermal conductivity. Although it is widely accepted that defected microstructure made up of pores and cracks contribute substantially to the reduced thermal conductivity of YSZ TBC coatings, *vertical* and in particular *segmentation* cracks are extensively reported to produce the opposite effect. In fact, the thermal conductivity of coatings with high *segmentation* cracks density can rise up to 50% [16]. This is because the contribution of the flow of high temperature gas into the pores to heat transfer makes more significant [13]. Recent FEM modeling of TBCs has also confirmed the dominant role of the longest transverse crack to the thermal conductivity of the coating when compared with any individual defect [17].

The findings obtained allow confirming some of the previous research carried out with YSZ TBC coatings obtained by APS processes which have been extensively treated in the literature due to their industrial applications. However further research is still necessary so as to better understand the correlation between microstructure and thermal properties in SPS coatings since as widely recognized nanostructured YSZ coatings show clear potential to become part of the next generation of TBCs.

4. Conclusions

3YSZ coatings were obtained by SPS from an aqueous commercial suspension. Thermal diffusivity was measured using commercial NanoFlash system in the temperature range from room temperature to 573 K. Thermal conductivity was then calculated from thermal diffusivity measurements. The different types of cracks were identified by SEM inside the coating microstructure namely; *inner* microcracks and *segmentation* cracks associated with splat quenching process and *horizontal* interlamellae cracks.

Very low thermal conductivities values were obtained which did not correlate with coatings porosity data. ANOVA test was performed to try to relate these types of cracks identified in the coatings with thermal conductivity values. A good correlation between *vertical* cracks which include *inner* microcracks and *segmentation* cracks and thermal conductivity was found. The findings also confirmed the increase of thermal conductivity associated with this type of cracks as reported in the literature.

Acknowledgments

This work has been supported by the Spanish Ministry of Science and Innovation (project MAT2009-14144-C03) and the Research Promotion Plan of the Universitat Jaume I, action 2.1 (ref. E-2011-05) and action 3.1 (ref. PREDOC/2009/10).

References

1. Padture NP, Gell M, Jordan EH. Thermal barrier coatings for gas-turbine engine applications. *Science* 2002;296:280-4.
2. Tian YS, Chen, CZ, Wang DY, Ji Q. Recent developments in zirconia thermal barrier coatings. *Surf Rev Let* 2005;12:369-78.
3. Curry N, Markocsan N, Li XH, Tricoire A, Dorfman M. Next generation thermal barrier coatings for the gas turbine industry. *J Therm Spray Technol* 2011;11:108-15.
4. Wang Y, Wu W, Zheng X, Zeng Y, Ding M, Zhang C. Relationship between the microstructure and thermal conductivity of plasma-sprayed ZrO₂ coatings. *J. Therm Spray Technol* 2011;20:1177-82.
5. Tan Y, Srinivasan V, Nakamura T, Sampath S, Bertrand P, Bertrand G. Optimizing compliance and thermal conductivity of plasma sprayed thermal barrier coatings via controlled powders and processing strategies. *J Therm Spray Technol* 2012;21:950-62.
6. Pawłowski L, Fauchais P. Thermal transport properties of thermally sprayed coatings. *Int Mater Rev* 1992;37:271-89.
7. Fauchais P, Montavon G, Lima RS, Marple BR. Engineering a new class of thermal spray nano-based microstructures from agglomerated nanostructured particles, suspensions and solutions: an invited review. *J Phys D Appl Phys.* 2011;44:093001.
8. Pawłowski, L. Suspension and solution thermal spray coatings. *Surf Coat Technol* 2009;203:2807-29.
9. H. Kassner, R. Siegert, D. Hathiramani, R. Vassen, D. Stoeber. Application of suspension plasma spraying (SPS) for manufacture of ceramic coatings. *J Therm Spray Technol* 2008;17:115-23.
10. VanEvery K, Krane JM, Trice RW, Wang H, Porter W, Besser M, Sordelet D, Ilavsky J, Almer J. Column formation in suspension plasma-sprayed coatings and resultant thermal properties. *J. Therm Spray Technol* 2011;20:817-28.
11. Carpio P, Rayón E, Pawłowski L, Cattini A, Benavente R, Bannier E, Salvador MD, Sánchez E. Microstructure and indentation mechanical properties of YSZ nanostructured coatings obtained by suspension plasma spraying. *Surf Coat Technol* <http://dx.doi.org/10.1016/j.surfcoat.2012.09.047>
12. Lide DR. *CRC handbook of chemistry and physics*. 88th. Boca Raton: CRC;2008.

13. Golosnoy IO, Cipitria A, Clyne TW. Heat transfer through plasma-sprayed thermal barrier coatings in gas turbines: a review of recent work. *J Therm Spray Technol* 2009;18:809-21.
14. Vassen R, Kassner H, Mauer G, Stoeber D. Suspension plasma spraying: process characteristics and applications. *J Therm Spray Technol* 2010;19:219-25.
15. Bacciochini A, Ben-Ettouil, F. Brousse E, Ilavsky J, Montavon G, Denoirjean A, Valette S, Fauchais P. Quantification of void networks of as-sprayed and annealed nanostructured yttria-stabilized zirconia (YSZ) deposits manufactured by suspension plasma spraying. *Surf Coat Technol* 2010;205:683-89.
16. Hongbo G, Kuroda S, Murakami H. Microstructured and properties of plasma-sprayed segmented thermal barrier coatings. *J Am Ceram Soc* 2006;89:1432-39.
17. Wei S, Fu-chi W, Qun-bo F, Zhuang M. Effects of defects on the effective thermal conductivity of thermal barrier coatings. *Appl. Math. Modelling* 2012;36:1995-2002.

Figure captions

Figure 1. FEG-SEM cross section micrographs (sample 2 from reference [11]).

Figure 2. Different types of cracks identified by image analysis from the original micrograph of sample 5 (reference [11]).

Tables

Sample	Spray parameters		Type of cracks (%)			Thermal conductivity (W/(m·K))	
	Linear speed (mm/s)	Injection pressure (bar)	Segmentation	Inner	Horizontal	T=50 °C	T=300 °C
1	250	1.5	2.16	3.18	3.63	1.34	1.3
2		3.5	-	2.33	2.33	0.68	0.56
3	300	2	-	1.38	3.70	0.54	0.43
4	350	1.5	-	1.72	1.98	0.60	0.52
5		3.5	2.74	2.34	4.36	0.85	0.85

Table 1. Spray parameters, cracks percentage and thermal conductivity of the coatings (samples reference from [11]).

Case	Degree of freedom	Critical F	Variables (type of cracks)	Coefficients	Error (%)	R ²
1	1	0.37	Segmentation	0.048	401	0.91
			Inner	0.392	65	
			Horizontal	0.046	429	
2	2	0.14	Vertical	0.193	33	0.86
			Horizontal	-0.070	173	
3	3	0.03	Vertical	0.170	26	0.83

Table 2. Correlation coefficients and results of the ANOVA test.

Figure 1
[Click here to download high resolution image](#)

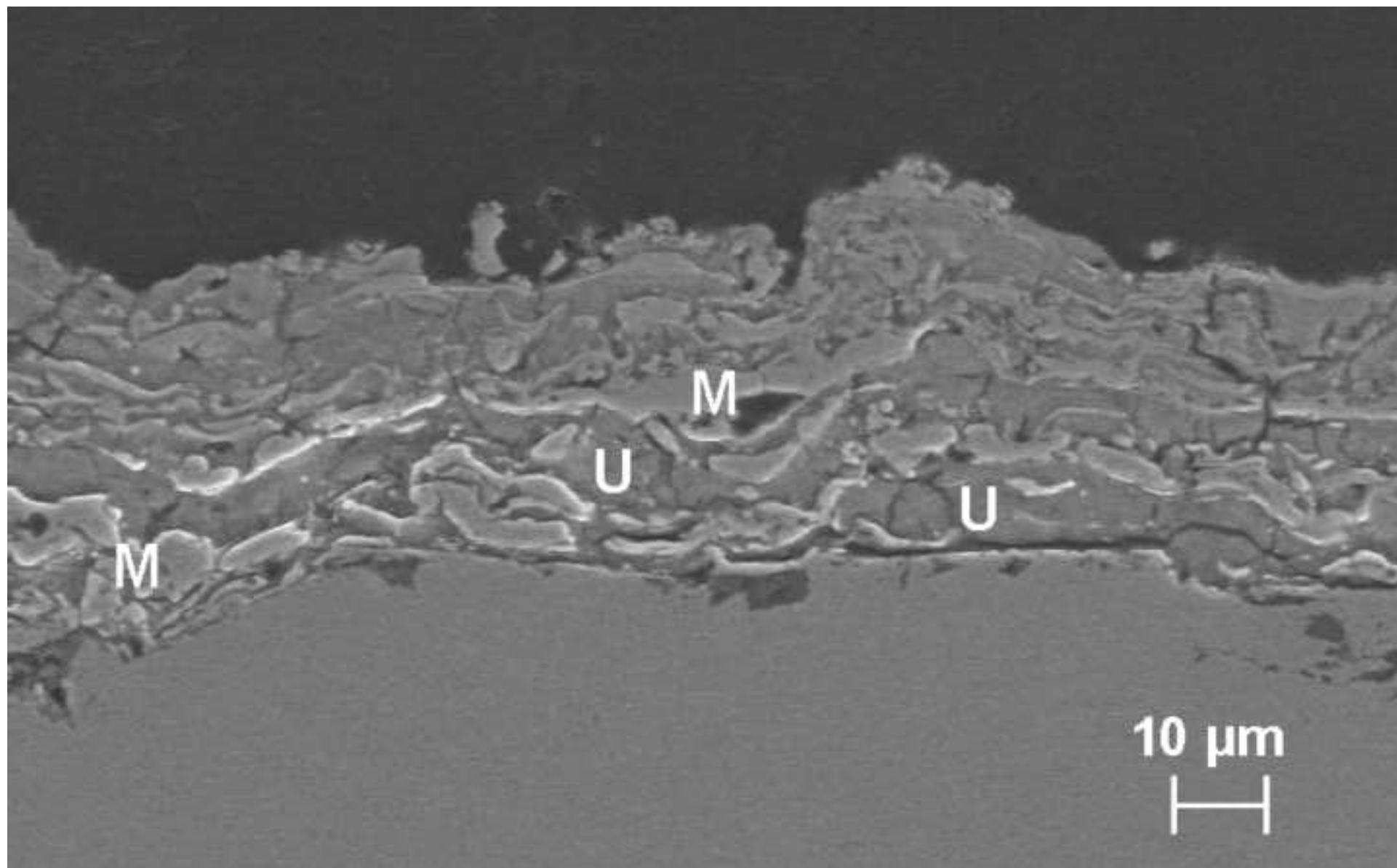


Figure 2
[Click here to download high resolution image](#)

